Blue twilight in a simple atmosphere

Phil Ekstrom

Lotek Wireless 114 Cabot St., St. John's, NF, A1C 1Z8 Canada
CEFAS, Pakefield Rd. Lowestoft, Suffolk NR33 0HT, England

ABSTRACT

Assuming a curved exponential atmosphere with beam attenuation and isotropic scattering both proportional to density, we model three regimes that each become dominant in turn as the sun sets. This drastic simplification of the earth's real atmosphere both provides insight to guide system design and is able to fit over an irradiance range exceeding nine decades a set of narrowband measurements of blue light intensity made in the natural environment on clear days. The single-scattering regime involves only overall illumination (or cloudiness) as an adjustable parameter and appears especially relevant to animal geolocation based on measurement of diffuse irradiance.

Keywords: Twilight, Blue Twilight, Scattering, Geolocation, Atmosphere

1. INTRODUCTION

Work on determining geographic position from measurements of diffuse natural light intensity has been hampered by the lack of any satisfactory and accessible model of atmospheric processes affecting the light being measured. This is serious since an essential step in the geolocation process is an inference from measured irradiance to elevation angle of the sun. Recent analyses of geolocation[1] proceed as if they were dealing with the direct beam of the sun even under conditions when it seems clear that scattered light is already dominant.

While investigations of sky brightness abound,[2] they do not treat the issues at stake in geolocation, are typically oriented toward numerical tabulation rather than analytic results and in fact have had no impact on animal geolocation work. In response to this situation, we report here a simple physical model that can reproduce the observed intensity of total illumination measured on a clear day in a narrow spectral band of blue light from daytime into deep twilight. Those results are also relevant to cloudy days in a sense that will be discussed. Throughout, every effort is made to pursue insight and achieve analytic results as a basis for designing geolocation instruments.

While much of the formalism applies equally to any wavelength, many of the approximations made have high accuracy only for blue light, comparison data were taken in the blue (470nm), parameter values assumed are appropriate to that spectral range, and many of the comments and conclusions depend on the comparatively strong scattering that is observed in our real atmosphere in the blue. When doing measurements for geolocation, especially in ocean fish, there is good reason to confine one's attention to the blue. Not only does blue light penetrate deepest in the open ocean[3] and permit the simplest corrections for attenuation by the water[4], but also the results to be obtained below point out the advantages of strong absorption and scattering in the atmosphere that blue light experiences.

2. THE MODEL ASSUMPTIONS

We assume that

1) The earth is spherical with radius R. That is, we do not make the convenient flat-earth approximation to path length, and we initially assume no clutter on the horizon. R = 6378km.

2) The atmospheric density is exponential with height y above the earth's surface. That is, $\rho(y) = \exp(-y/s)$ where s is the density scale height and the density at the earth's surface is taken to be unity. $s \approx 6.35$km.[5]
3) Parallel light from the sun is incident on the atmosphere with irradiance E_0 at an elevation angle a with respect to the surface where the observer is.
4) That direct beam from the sun is refracted toward the earth's surface in passing through the atmosphere. The total angle of refraction at a=0 and for an observer at altitude h is approximately $0.53° \rho(h)$.[6]
5) Light is attenuated at a rate proportional to the local atmospheric density. That is, $dE/dl = -\alpha\rho(h)E$ where dl is an element of length in the direction of propagation and α is a constant, the inverse attenuation length at zero altitude.
6) Some fraction of that light lost from the beam is scattered isotropically, and this isotropic component dominates the scattering at large angles of deviation from the beam direction. That is, the radiant intensity scattered at large angles per element of solid angle $d\Omega$ can be written as $dI/dl\, d\Omega = \beta\rho(h)E/4\pi$, where β is a constant.
7) All other scattering is predominantly in the forward direction. Light so scattered is in most cases treated as not having been removed from the direct beam.
8) Horizon clutter and clouds, otherwise excluded by the previous assumptions, may be introduced *ad hoc* in situations where their effects can be evaluated *ad hoc*.

3. REGIME 1: THE DIRECT BEAM

When the sun is high in a clear sky, the earth's surface is dominantly illuminated by light traveling in a nearly straight line from the sun to the observer, but absorbed and scattered along the way. We model the resulting attenuation here.

Consider a ray of light approaching a point on the surface of the earth along a path that makes an elevation angle, conventionally denoted by the letter a, with the local surface at the observing point. In particular consider a point on that path a slant distance z from the surface. With reference to the diagram, we may make the excellent approximation that $y<<2R$ for any point within the atmosphere and write the height of that point above the nearest surface as $y \approx z \sin(a) + z^2/2R$.

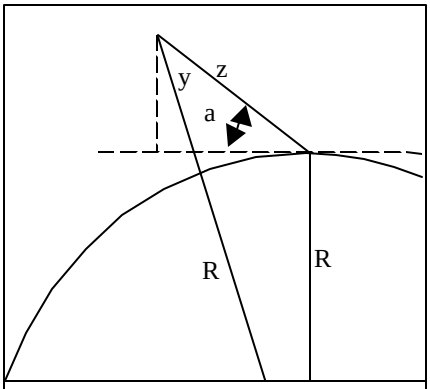

Fig 1. Geometry for direct beam.

Assumptions 2 and 3 lead directly to the differential equation for beam intensity $dE/dz = -\alpha E \exp(-y/s)$, which on substituting for y and integrating from $z = -\infty$ to 0 becomes $\ln(E) - \ln(E_0) = -\alpha \int \exp(-z(\sin(a) + z/2R)/s)\, dz$. The remaining integral can be done with reference to standard tables, and leads to

$$E_1 = E_0 \exp(-\alpha L(a)) \quad \text{where for } a \geq 0 \qquad (1a)$$

$$L(a) = \sqrt{(\pi s R/2)} \exp(u^2) \operatorname{erfc}(u) = 252\text{km} \cdot \exp(u^2) \operatorname{erfc}(u) \text{ and} \qquad (1b)$$

$$u = \sqrt{(R/2s)} \sin(a) = 22.4 \sin(a) \qquad (1c)$$

.

L is the effective path length, so far defined only for positive values of a.
Over that domain it is equal to the quantity plotted in Fig. 5 below. For a blue-light attenuation parameter of $\alpha \approx 0.035$ km^{-1}, the beam attenuation to the surface at geometric sunset is $\exp(-\alpha L(0)) \approx \exp(-9.2) \approx 10^{-4}$. No significant amount of direct-beam blue light is present at the surface just at geometric sunset.

The actual evaluation of L requires care at large positive a, where the exponential term becomes very large and the error function complement becomes correspondingly small. Both can exceed the range of a computer floating-point representation, despite the fact that their product is well behaved. For sufficiently large elevation angles, a > 8 degrees, one can instead use the "flat earth" approximation $L(a) \approx s/\sin(a)$.

When we use this result to calculate the irradiance incident on a horizontal surface or a horizontal Lambertian detector, we must multiply the result given above by an additional geometric factor sin(a). When calculating the irradiance illuminating a scattering volume or a spherical detector, the unmodified expression is appropriate.

4. REGIME 2: SINGLY-SCATTERED LIGHT (PRIMARY TWILIGHT)

The surface is also illuminated by light that is scattered in the atmosphere, resulting in a blue sky and daytime shadows that are not completely black. In this section we evaluate its irradiance at the surface.

4.1 The case a>0: before geometric sunset

Incident light first travels part way to the surface along a path like the one considered above but not leading all the way to the surface. Then, after scattering, it travels away from the scattering point along some different path. Thus the diagram at the right differs from the similar one above in that the direct beam penetrates the atmosphere only as far as altitude h before being scattered. In the calculation of direct beam intensity, the height y appearing in the equations above may be replaced by y + h. That is equivalent to replacing α by $\alpha\rho(h)$ with the result that the illumination intensity at the scattering point is $E_1 = E_0 \exp(-\alpha\rho L)$ where $\rho = \exp(-h/s)$, and L is just as above.

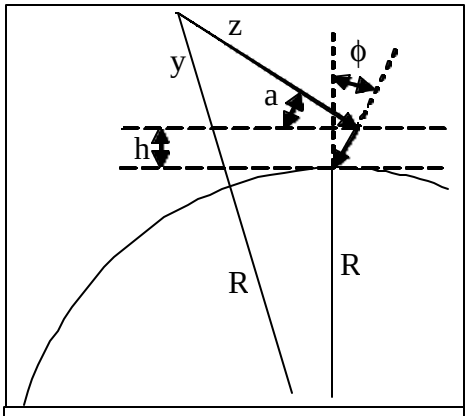

Fig 2: Geometry for single scattering with elevation angle positive

According to model assumption 6, this results in an intensity of scattered light equal to $dI_2/dl\, d\Omega = \beta\rho(h)E_1/4\pi$

Scattered light from a localized volume in the atmosphere at an altitude h above a given observation point will reach the ground making some zenith angle ϕ with the local vertical. We have again the path attenuation problem we had earlier, with two differences. First, large zenith angles (small elevation angles) will here make a negligible contribution to the intensity so we can neglect the curvature of the atmosphere and take the path length to be $s/\cos(\phi)$. Second, most of the beam attenuation described by the parameter α is not absorption, but scattering out of the beam. In this case with a diffuse source that scattered light is not lost, but rather redistributed and much of it will reach the surface. Therefore, we approximate the diffuse rate as the difference $\alpha-\beta$. Under these conditions we obtain a simpler result that the ray is attenuated by a factor $\exp[-(\alpha-\beta)\cdot(1-\rho)\cdot s/\cos(\phi)]$.

Now consider an atmospheric shell at altitude h and thickness dh illuminated by the incident ray of intensity E_1, and write the scattered energy flux associated with a scattering volume in that layer of cross sectional area dA_1 normal to the beam and of thickness dl. It is just the intensity result above, times the cross sectional area dA_1.
In all, $d\Phi_2 = E_1\, \beta\, \rho\, \exp(-\alpha s\,(1-\rho)/\cos(\phi))dl\, dA_1\, d\Omega/4\pi$ Preparing to integrate this result over the entire scattering layer, we transform the differentials to $dh\, dA_2\, d\omega$, where $d\omega$ is the solid angle subtended by the scattering volume as seen from the observing point on the ground. Noting that $d\Phi_2/dA_2 = E_2$, the irradiance seen on the ground, we can write $dE_2 = E_1\, \beta\, \rho\, A(p)dh$ where $p=(\alpha-\beta)\cdot s\cdot(1-\rho)$ and $A(p) = \iint \exp(-p/\cos(f))dw/4p$ or

$$A(p) = (1/2)\int_0^1 \exp(p/x)dx \qquad (2)$$

The function A(p) is plotted at the right over the range $0 < p < 1.5$ which covers all cases for $\alpha-\beta < 0.25$. Qualitatively what is occurring as p increases is that the longest paths corresponding to the largest values of ϕ quit contributing and the surface can only "see" the scattering layer more and more directly overhead. Light from the zenith is attenuated by a factor exp(-p).

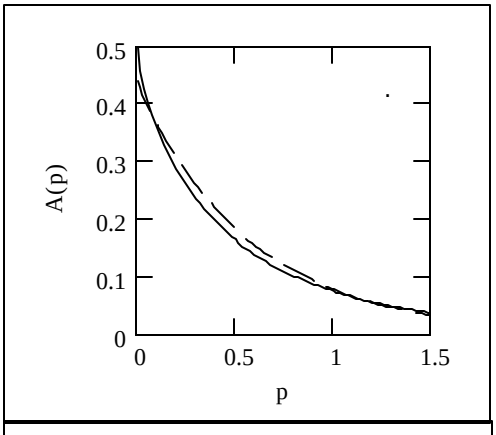

Fig 3. Attenuation Integral. Dashed line is the exponential approximation.

Below it will become convenient to have an exponential approximation to this function. The one shown by the dashed line in the figure is

$$A(p) \approx 0.44 \exp(-1.75p). \qquad (3)$$

Substituting the results we have so far yields $dE_2 = E_0 \cdot \exp(-\alpha\rho\ L) \cdot \beta \cdot \rho \cdot A((\alpha-\beta)s(1-\rho))\ dh$. To obtain E_2 we will need to integrate over h. When full accuracy is needed that integral will be done numerically, but an analytic approximation will be offered after we treat the second half of this regime.

4.2 The case a<0: after geometric sunset

When the sun elevation angle a becomes less than zero, the sun has set and the geometric situation changes, as illustrated in the drawing at the right. We now turn to this second case in the singly-scattered regime.

A ray from the sun first achieves its minimum altitude h above one location on the earth's surface, then continues on to the scattering point a distance x beyond. Light scattered there finally reaches the earth an angular displacement a beyond the point of closest approach. There are two new effects as we follow the ray out through its extended trajectory: the path length and consequent absorption increases along a path of any given minimum height h, and the scattering height increases above h, bringing with it a decreased atmospheric density. Both effects tend to reduce the irradiance seen on the ground.

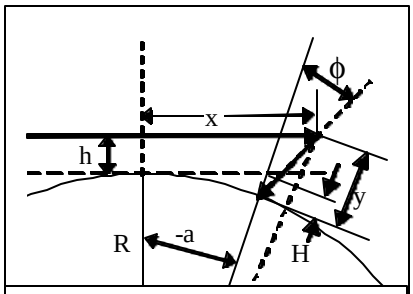

Fig 4. Geometry for single scattering with a<0.

To investigate both effects we need an expression for height y as a function of **a**. Although the altitude h and the angle a have been drawn large for clarity, we are actually concerned here only with small angles a such that $\sin(a) \approx a$ and $\cos(a) \approx 1$, and with small h such that $h << R$. These approximations lead to $y = (R+h)\sec(-a) - R = h + H$ where $H \approx R(\sin^2 a)/2$.

Attenuation along the extended path can be integrated as before to yield $E = E_1(h) \cdot \exp(-a\rho(h)L'(-a))$ where $L'(a) = \sqrt{(\pi s R/2)}\ \mathrm{erf}(\sqrt{(R/2s)}\sin(-a)) = L(0) \cdot \mathrm{erf}(u)$. The irradiance E_1 is just that at the point of closest approach, or $E_1 = E_0 \exp(-\rho(h)L(0))$. We can combine this case with the previous one by writing for the irradiance at the scattering point of the direct beam in terms of its distance of closest approach h as

$$E = E_0 \exp(-\alpha\rho(h)L(a)) \text{ where} \qquad (4a)$$

$$L(a) = \sqrt{(\pi s R/2)} \exp(u^2)\ \mathrm{erfc}(u) \quad \text{if } u \geq 0 \qquad (4b)$$

$$L(a) = \sqrt{(\pi s R/2)}\ (1 + \mathrm{erf}(u)) \quad \text{if } u < 0$$

$$\text{where } L(0) = \sqrt{(\pi s R/2)} = 252 \text{ km}, \quad u = \sqrt{(R/2s)}\ \sin(a) = 22.4 \sin(a) \qquad (4c)$$

The resulting extended definition is plotted at the right. The two half-curves merge smoothly at a = 0.

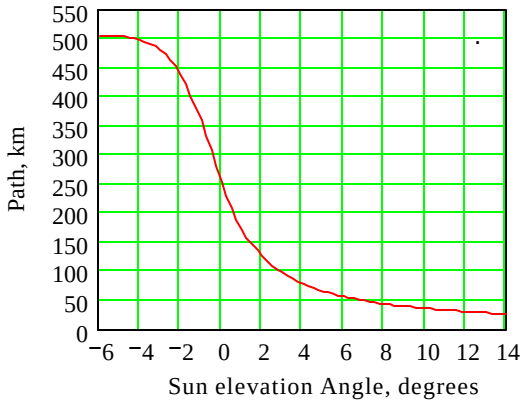

Fig 5. Path Length, extended definition

We also define the scattering height

$$h_s = h + H \text{ where} \qquad (5a)$$

$$H = 0 \qquad a \geq 0 \qquad (5b)$$

$$H = R \cdot \sin^2(a)/2 \qquad a < 0.$$

Proceeding along the lines pursued for regime 2a, we make the small-angle approximation freely, and the details go through just as before, except that we use the extended definition of L and distinguish between the height of closest approach h and the scattering height h_s.

For all small angles a the result becomes

$$dE_2 = E_0 \cdot \exp(-\alpha\rho(h)\ L(a))\ \beta\ \rho(h_s)\ A[(\alpha-\beta) \cdot s \cdot (1-\rho(h_s))]dh \quad (6)$$

4.3 A note on atmospheric refraction and horizon clutter.
Here we evaluate the expected effect of atmospheric refraction and horizon clutter, finding them to be insignificant for blue light and elevation angles less than 3°.

Plotted vs. h at the right is the quantity dE_2/dh for a typical value of α and several choices of elevation angle a. The scattered contribution falls off at low altitudes because at these low elevation angles most of the blue light is absorbed before it reaches the surface. It falls off at high altitudes as the atmospheric density and the density of scatterers decreases. As the elevation angle a decreases and the path length L increases, the peak moves upward.

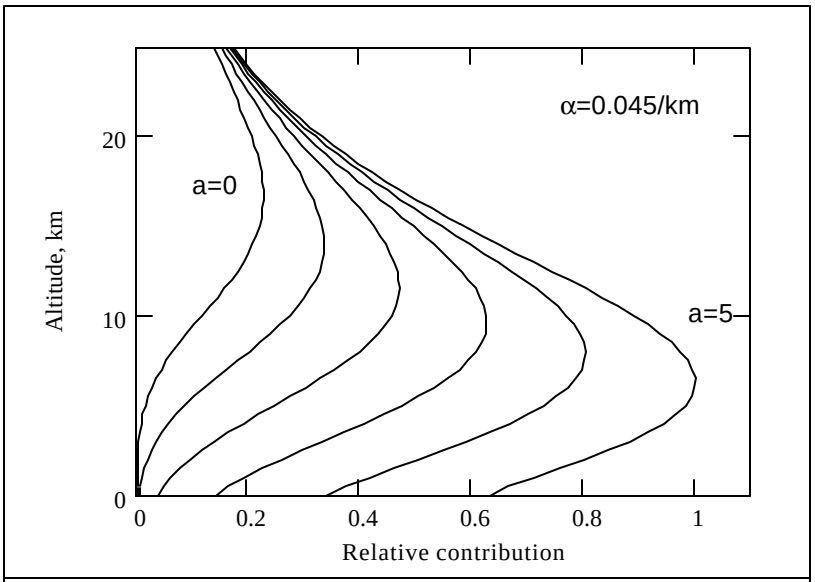

Fig. 6. Scattering contribution vs. height for a = 0, 1, 2, 3, 4, and 5°

For a=0, the peak is at h = 16.5 km, where the atmospheric density is only $\rho = \exp(-h/s) = \exp(-2.4) \approx 0.09$. The scattering process that is intercepting the direct beam is centered at an altitude above 90% of the atmosphere. Accordingly, any process like refraction that is proportional to atmospheric density at the observer's location will be reduced by that same factor of 0.09. The nominal 0.53° beam deviation seen at sea level is reduced to approximately 0.05° at the peak of the scattering distribution, and is therefore not a significant limit to the geolocation accuracy presently attainable.

Similarly, since most of the scattering is driven by rays that never come close to the surface, we find that the light curve is largely independent of any horizon clutter no more than a few km high in all those cases where scattered light dominates and where the scattering rate α is sufficiently large.

We can learn more about atmospheric density at the scattering peak by substituting the exponential approximation for A(p) to yield $dE_2/dh \approx A(\alpha s)\, \beta\, E_0\, \rho \exp(-\rho\, (\alpha L - 1.75((\alpha-\beta)s\rho(H))$. We can locate the peak of this function in the usual way by differentiating with respect to ρ and setting the result to zero. We find that the peak occurs where $\rho(\alpha L - 1.75(\alpha-\beta)s\rho(H)) = 1$, or approximately where $\alpha\rho L \approx 1$. This approximate relation predicts $\rho = 1/\alpha L$ which is again about 0.084 for α=0.045 and a = 0. There is a useful qualitative insight to be had here: since the attenuation of the direct beam at any given point is $\exp(-\alpha\rho L)$, we see that the direct beam always encounters an attenuation by a factor of e on its way to altitude where the scattering contribution peaks. If the atmosphere becomes dustier or as noted above if the elevation angle decreases, the scattering peak moves higher.

4.4 Interpretation of dE_2 and its approximate integral – Rigidity of the singly-scattered light curve.
Beginning again with the approximate expression for E_2 developed just above, we note that $\rho\, dh = -s\, d\rho$ and integrate with respect to height in terms of ρ. The result is

$$E_2 \approx E_0\, [1-\exp(-\alpha L(a) - 1.75(\alpha-\beta)s\rho(H))]\, (\beta/\alpha)\rho(H)\, (s / (L(a) - 1.75(\alpha/\beta - 1)s\rho(H)))\, A((\alpha-\beta)s). \qquad (7)$$

Each factor in this expression has an interesting interpretation. E_0 represents the insolation, while the term in square brackets is approximately the fraction of the insolation that is absorbed and scattered before reaching the ground. When α is sufficiently large and the elevation angle a sufficiently small, the exponential factor can be neglected. For example

when α= 0.04 and a = 3°, the exponential factor is less than 0.03 and the bracket greater than 0.97; that is, less than 3% of light the direct beam reaches the ground and for practical purposes we may replace the square bracket by 1. In just that case this factor no longer influences the shape of the light curve.

The factor β/α is the fraction of the direct beam that is scattered as opposed to absorbed. The factor $\rho(H)$ is 1 when the sun is above the horizon, but it contributes a term $\exp(-\sin^2(a)\, R/2s)$ which is Gaussian in angle for all a<0. It accounts for the continued increase into deep twilight of the steepness of the predicted light curve. The term $(s/(L(a)-1.75(\alpha/\beta-1)s\rho(H)))$ is approximately the fraction of the scattering that occurs "overhead", and $A((\alpha-\beta)s)$ is the fraction of that scattered light which would reach the ground from a scattering layer above most of the atmosphere. In each factor where it occurs, the term $1.75s\rho(H)$ arises in the details in a way that suggests it as a correction to $A(\alpha s)$ for the actual height of the peak, which is not above all the atmosphere.

When scattering is sufficiently strong, the exponential term can be neglected and there is no longer any term that mixes a and α in a way that can affect the shape of the light curve; that shape becomes independent of α so long as $\alpha L(a)$ is sufficiently large. This gift of sufficiently strong scattering is a substantial advantage when making the inference from intensity variations during twilight to the causative variations in sun angle.

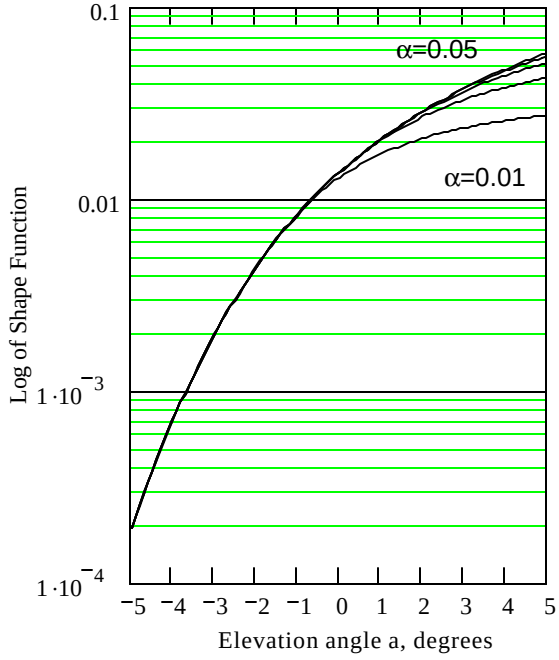

Fig. 7: Light curve in single-scattering regime for α = 0.01, 0.02, 0.03, 0.04, and 0.05 km^{-1}.

The figure at the right plots the quantity $E_2/ 2A((\alpha-\beta)s)$ E_0 (β/α), which expresses that shape, vs. the elevation angle a for several values of α. This data is based on a full numerical integration of dE_2. Note that, as predicted by the approximate calculation, the shape of the curve stabilizes for all a<3° when α>0.04.

5. REGIME 3: DUCTED LIGHT (SECONDARY TWILIGHT)

Experimentally, the Gaussian behavior predicted by regime 2 is replaced in deep twilight by a simple exponential. In this section we suggest how this may arise and argue for a functional form. The approach will be less rigorous than previous sections, as this regime seems less interesting for the application at hand and the situation more difficult to treat in detail.

Portions of the atmosphere shielded from the direct beam of the sun can be illuminated indirectly by light from regions that are illuminated when light is forward-scattered so as to deviate by a small angle towards the surface. This is the "secondary twilight" referred to in the Russian literature[7]. That light which happens to be successively scattered at the correct angles to approximately match the curvature of the earth can in turn illuminate other regions of the atmosphere even further over the horizon. As the light is both absorbed in its travels and dispersed at each scattering, we expect that the intensity of this component will decay with distance from the geometric horizon. Once over the horizon, each new unit length of atmosphere presents the same situation and should attenuate the light by the same factor. The decay will be exponential in elevation angle.

We model this process as a continuous distribution of large-angle scattering events, treating each as if it were the single-scattering studied previously, except attenuated by an exponential factor proportional to its displacement over the horizon. There are two parameters to be determined heuristically, an overall intensity K and an angular scale factor **as**.

Again we take sin(t)≈t for t in radians.

$$E_3(a) = K\int_a^{a\max} E_2(t)\exp\left(-\frac{t-a}{as}\right)dt = K\cdot\exp\left(\frac{a}{as}\right)\cdot\int_a^{a\max} E_2(t)\exp\left(\frac{-t}{as}\right)dt \qquad (8)$$

Note that since a and t are increasingly negative in this regime, exp(-t) becomes larger and exp(a) becomes smaller as we go deeper into twilight. The upper limit of integration, shown above as amax, is relatively non-critical. Because of the exponential multiplying I_2, the integrand peaks sharply on the negative side of zero, and only a small range of angles contributes. Thus amax may have any convenient value larger than about 5 degrees, or 1/12 radian. Unfortunately the integral cannot be done analytically in terms of familiar functions, so we must approximate it numerically.

6. COMPARISON WITH FIELD DATA

Irradiance measurements were made in two locations using a filtered silicon photodiode driving a logarithmic current-to-voltage converter. The logarithm of detected irradiance was recorded at a resolution of 15 units per decade.[8] The wavelength filter and light diffuser is a patented arrangement involving a plastic optical fiber doped with a fluorescent dye. The spectral response of the detector is set by the excitation spectrum of the dye, and is shown in Fig. 8.

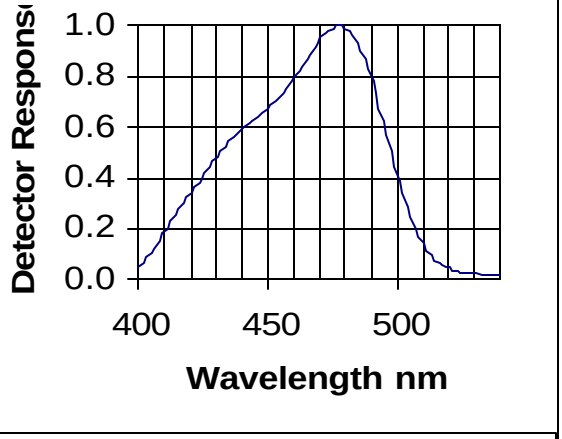

Fig 8: Spectral response of detector.

The first measurement station was a few miles east of Pasco, WA, USA in an area with a good horizon, but with the sky illuminated at night by lights from the nearby city. The optical fiber that is the effective sensor was oriented parallel to the polar axis of the earth, so that we have a nearly angle-independent detector instead of a Lambertian one. In addition, there was an occulting band provided to place the detector in shadow for a few minutes near noon of each day. Data from a particular clear day is shown in Fig 9, plotted against sun angle calculated from the known location, season, and time-of-day. Also shown are model curves best-fit to the data. Fitting was done by eye, beginning with secondary twilight, adding the single-scattering curve, and finally adding the direct beam. Each successive regime was fit to the region where it dominates. Parameters adjusted were $K/\beta E_0$ and the angular scale as for secondary twilight, βE_0 and α for single-scattering or primary twilight, and E_0 for the direct beam. For this fit, the angular scale for ducted light was 1 degree, α = 0.035 and β=0.035. Note that the total-scattered curve does not pass through the data affected by the occulting band shadow. Presumably that shadow was illuminated by forward-scattered light not taken into account by the model.

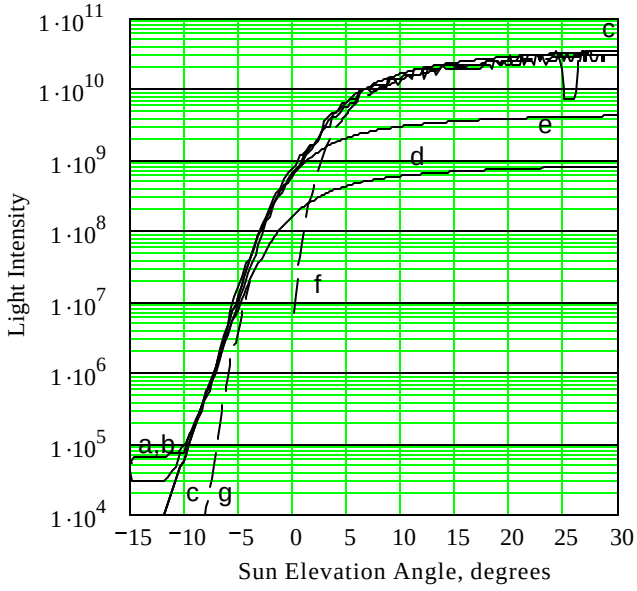

Fig. 9: Pasco data plus model curves. a,b: sunrise and sunset data, c:(labeled both ends) full model, d: multiply scattered, e: total scattered, f: direct beam, g: singly scattered (for a<0)

The second station was in a forest clearing on Shaw Island, WA, USA. In exchange for its much darker sky, this site has a horizon obscured by trees. In the clear-day data of Fig 10 one can see the trees interrupting the direct beam at small

positive sun angles much as the occulting band did at large angles in the previous record. Measured intensities tend to lie on the single-scattering curve when the detector is in shadow. For this fit, the angular scale was 0.8 degree, α=0.05 and β=0.037.

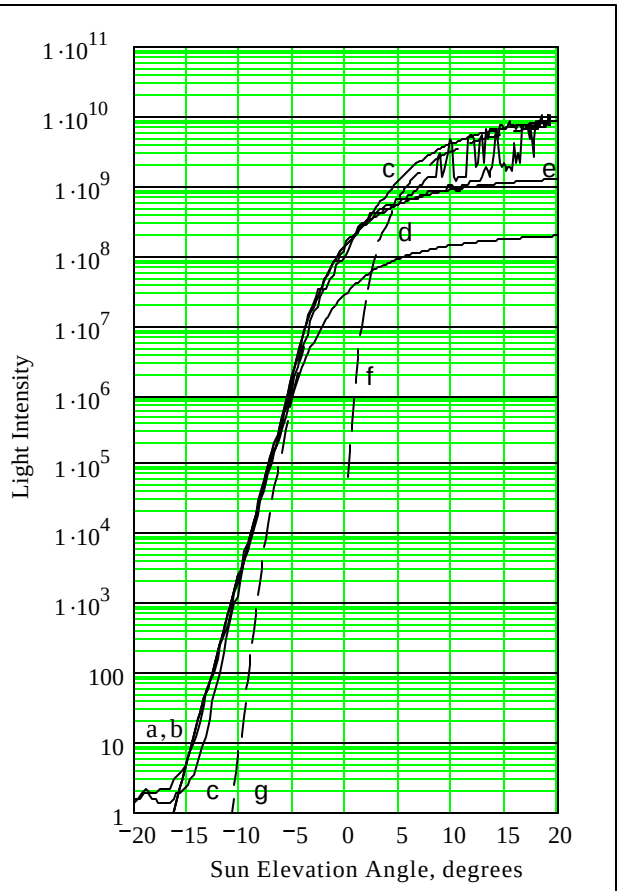

Fig. 10: Shaw data plus model curves. a,b: sunrise and sunset data, c:(labeled both ends) full model, d: multiply scattered, e: total scattered, f: direct beam, g: singly scattered (for a<0)

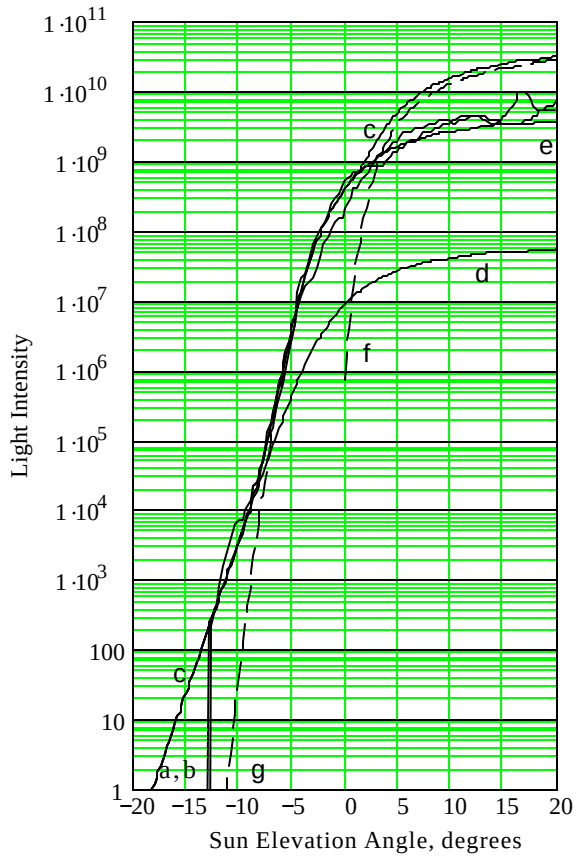

Fig. 11: Shaw data from a cloudy day plus model curves. a,b: sunrise and sunset data, c: full model, d: multiply scattered, e: total scattered, f: direct beam, g: singly scattered (shown only for a<0).

Since we have shown that most of the scattering involved in the single-scattering (primary twilight) regime occurs above most clouds, one expects the shape of the light curve in that regime to be largely independent of cloudiness whenever the cloud cover does not change during the sunrise or sunset transient. Figure 11 shows data from a cloudy day at the Shaw site measured by a different instrument of a similar type. The sudden break in the data at -13° elevation angle is an artifact of the instrument, and represents its effective sensitivity floor. The day was chosen as an extreme case in a separate study that compared irradiance at noon with irradiance measured at geometric sunset. The region from –5° to +3° sun elevation angle can indeed be fit reasonably well for one of the transients, though somewhat less well for the other. Although there is no independent verification of this, it seems reasonable to assume a greater change in the cloud layer in one case when compared to the other. Since there is no time during the day when the direct beam reached the instrument, α was arbitrarily assigned the same value found in the case of Fig 10.

7. DISCUSSION

The apparent success of this model in fitting field data certainly does not mean that the atmosphere really is as simple as assumed here. It is well known not to be. For one example there is no known isotropic scattering mechanism to be found in the real atmosphere.

What the success does mean is that broad features of the situation do not depend sensitively on details of the scattering processes. In particular, one key result is that so long as beam attenuation α is sufficiently large, the peak of the single-scattered contribution is located at an altitude where an incident ray is attenuated by 1/e. Because of the way that it arises in this simple model, one suspects that this is a feature that is likely to persist in the real atmosphere. That result in turn lies behind the remarkable properties deduced for the single-scattering regime in the case of strong scattering.

The central result of this paper is that a rigid shape is predicted for the blue-light single-scattering regime, and that it does actually fit field data over a range of angles that ordinarily includes $-5° \leq a \leq 3°$.

Two additional blue-light results run counter to received wisdom in the field of animal geolocation. First: horizon clutter on a scale smaller than several km high does not have any significant effect on that light curve. Second: atmospheric refraction can contribute only about 1/20 degree of longitude error. In blue light, neither of these sources can cause geolocation errors that would impair currently achieved accuracy levels.

Although the model does not specifically include clouds, it does predict that most of the scattering occurs above the level of most clouds. This leads one to expect that a static cloud layer will ordinarily contribute an additional overall attenuation largely independent of sun angle. If that is the case, clouds would also not significantly affect the shape of the sunrise-sunset transient unless the sky-averaged cloud density changed significantly during the transient. To the extent that this is the case, a geolocation method that sought to fit a template for that region to observed field data could potentially achieve substantial independence from the degree of overall cloud cover.

---

[1] Welch, D.W and Eveson, J.P. (1999) "An assessment of light-based geoposition estimates from archival tags". *Can. J. Fish Aquat. Sci*. **56**, 1317-1327
Hill, Roger and Braun, Melinda. "Geolocation by light levels – the next step: latitude". In *Electronic Tagging and Tracking in Marine Fisheries*, John Sibert and Jennifer Nielsen, eds., pp315-330, Kluwer, Boston (2001)

[2] Divari, N.B. and Plotnikova, L.I., "Computed Brightness of the Twilight Sky", Soviet Astronomy-AJ, **9**,840-852, (1966)
Belikov, Yu. E., "Modeling of the twilight sky brightness using a numerical solution of the radiation transfer equation". *Journal of Atmospheric and Terrestrial Physics*, **58**, 1843-1848 (1996)

[3] Pickard, G.L. and Emery, W. J., *Descriptive Physical Oceanography*, Pergamon, New York(1982)

[4] Ekstrom, P.A. "Inferring surface irradiance from measurements made at depth", (in preparation)

[5] Approximating the ICAO 1976 standard atmosphere model over 10 to 60 km altitude.

[6] *The Astronomical Almanac*, US Government Printing Office.

[7] Divari, N.B., ibid

[8] Archival Tag V1.1, Northwest Marine Technology, Inc. This product is no longer available, however the Lotek LTD2310 is a successor employing the same kind of detector. Lotek Wireless, 114 Cabot St., St. Jonn's NF A1C2B1, Canada. www.lotek.com